J. Membrane Biol. 154, 119–130 (1996)

The Journal of
Membrane
Biology

Effects of Polymyxin B on Mammalian Urinary Bladder

J.R. Berg, C.M. Spilker, S.A. Lewis
Department of Physiology and Biophysics, University of Texas Medical Branch, Galveston, TX 77555

Received: 9 May 1996/Revised: 17 July 1996

Abstract. Previous reports have demonstrated that large cationic polypeptides (of molecular mass 5,000 daltons or greater) cause an increase in the apical membrane conductance of the rabbit urinary bladder epithelium. This report investigates the effects of the small cationic molecule polymyxin B (PX: a 1,400 dalton antibiotic) on the permeability of the rabbit urinary bladder. The addition of micromolar concentrations of polymyxin B to the luminal solution of the rabbit urinary bladder resulted in an increase in the transepithelial conductance of the bladder. The magnitude of the increase in the conductance was dependent upon the concentration of PX, and the polarity and magnitude of the apical membrane potential. As the apical membrane potential was made more cell interior negative, the larger was the increase in the membrane conductance. This voltage-dependent increase in conductance was an exponential function of the applied voltage, with a negligible increase in conductance occurring when the membrane potential was cell interior positive. Upon changing the membrane voltage from cell interior positive to negative, there was a delay before there was a measurable change in the membrane conductance. The longer the apical membrane was exposed to PX, the more poorly reversible was its effect on the transepithelial conductance, suggesting a toxic effect of PX on this epithelium.

Key words: Polymyxin B — Cationic polypeptide — Bladder epithelium — Cytotoxicity — Nonselective conductance — Tight epithelium — Antibiotic

Introduction

There are a number of reports in the literature which suggest that cationic polypeptides (proteins containing significant quantities of the amino acids arginine and lysine) can be toxic to bacteria and parasites as well as mammalian cells. Among these cationic polypeptides are: the eosinophil proteins; major basic protein (MBP), eosinophil cationic protein (ECP) and eosinophil peroxidase (EPO) (Motojima et al., 1989); the neutrophil proteins cathepsin G, neutrophil cationic antimicrobial proteins CAP37 and CAP57 and the defensins (Spitznagel, 1990); the wheat germ purothionins and Holly viscotoxins (Carrasco et al., 1981); the magainins, a protein secreted from the skin of frogs (Zasloff, 1987); protamine, a nuclear compacting protein found in sperm (Tzan et al., 1993*a*; 1994, Teichman et al., 1994); as well as high molecular weight polypeptides composed of either or both arginine and lysine. Recent evidence suggests that ECP, defensins, magainins, protamine and purothionins cause an increase in the membrane ionic conductance of the target cells and perhaps prove cytotoxic by inducing cell swelling, followed by cell lysis.

In studies on the mammalian urinary bladder, Tzan et al. (1993 *a,b*) demonstrated that protamine (a 4,000-dalton protein composed of ≈67% arginine) or synthetic peptides composed of arginine or lysine, increased the apical membrane conductance of this epithelium. It was also shown that the magnitude of conductance increase was voltage dependent (a more cell interior negative voltage resulted in a larger conductance increase), that positive charge on the protein was essential to induce a conductance, as was a membrane binding site which catalyzed the increase in conductance.

In this communication, we investigate the effect of the cationic molecule, polymyxin B (PX) on the mammalian urinary bladder epithelium. Polymyxin B (Fig. 1) is an amphipathic cationic antibiotic, has a molecular mass of approximately 1,400 daltons, and contains five positive charges associated with the free amino group on the diaminobutyric acid molecule. It has been used clinically as a bactericidal agent during catheterization of the human urinary bladder. In brief, we demonstrate that

Correspondence to: S.A. Lewis

this molecule is able to increase the membrane ionic permeability of the urinary bladder in a manner similar to that of protamine or synthetic peptides composed of arginine or lysine. This increase in conductance was a saturating function of bath PX concentration and was dependent upon the polarity and magnitude of the membrane potential. Thus as the cell interior was made more negative, there was an increase in the transepithelial conductance. Such a sensitivity to membrane potential might explain why a molecule like PX is more toxic to gram negative bacterial cells than to mammalian cells. Lastly, evidence is supplied which suggests that PX is toxic to rabbit urinary bladder epithelial cells.

Materials and Methods

Urinary bladders from male New Zealand white rabbits were removed and the underlying smooth muscle layers dissected away according to the method of Lewis and Diamond (1976). The epithelium was then mounted in a temperature-controlled modified Ussing chamber designed to reduce edge damage (Lewis et al., 1977). Both mucosal and serosal solutions were aerated with 95% O_2 and 5% CO_2 and the solution stirred by magnetic spin bars driven by an external magnet coupled to a motor.

Solutions

The composition of the NaCl Ringers solution was (in mM): 111.2 NaCl, 25 $NaHCO_3$, 10 glucose, 5.8 KCl, 2 $CaCl_2$, 1.2 KH_2PO_4, and 1.2 $MgSO_4$. For the KCl solution, the Na^+ salts were replaced with the corresponding K^+ salts. Ca-Mg free Ringers was made by omitting the $MgSO_4$ and replacing the $CaCl_2$ with KCl. Unless otherwise stated the serosal bathing solution was NaCl Ringers and the mucosal solution was the Ca-Mg free KCl Ringers. Polymyxin B sulfate, which is composed of polymyxin B_1, and polymyxin B_2 (*see* Fig. 1), was from Sigma Chemical (St Louis, MO), and microliter quantities were added to the mucosal solution from a concentrated stock solution.

Electrical Measurements

The transepithelial potential (V_t) was measured using Ag/AgCl wires placed close to and on opposite sides of the epithelium. Current (I) was passed from Ag/AgCl wires placed in the rear of each hemichamber. The transepithelial conductance ($G_t = 1/R_t$) was determined by passing a current pulse across the epithelium and measuring the transepithelial voltage change (ΔV_t). Both the current passing and the voltage recording electrodes were connected to an automatic current/voltage clamp (EC-825LV, Warner Instruments, Hamden, CT).

The current and voltage outputs of the clamp were connected via a variable gain amplifier (LPF-202, Warner Instruments, Hamden, CT) to an analogue-to-digital converter (PP-50 LAB, Warner Instruments, Hamden, CT) which was interfaced to a laboratory computer. These parameters were digitized, stored on hard disk, and logged on a printer along with the time of data acquisition and the calculated values for R_t, G_t, and short circuit current at a maximum rate of one per second. In addition, V_t and I were continuously monitored on an oscilloscope and a paper strip chart recorder.

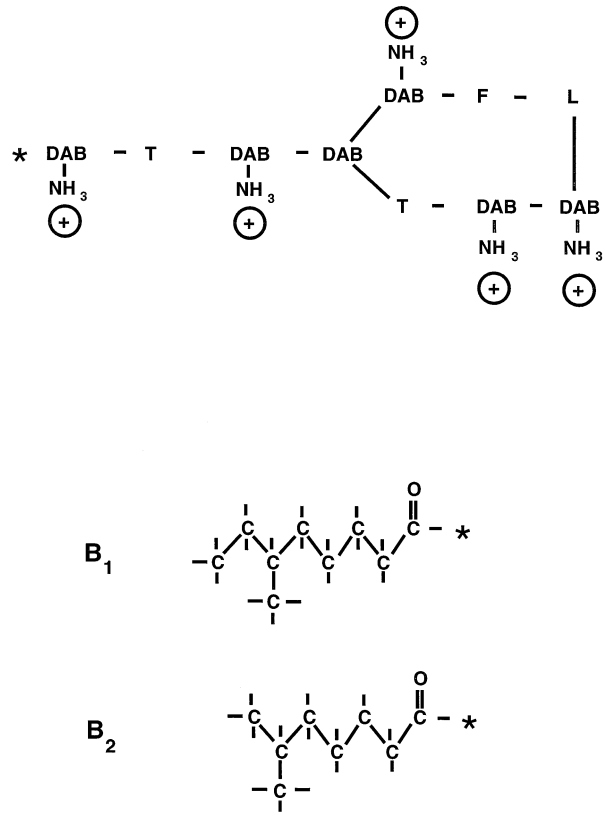

Fig. 1. Structure of polymyxin B. PX is a decapeptide with a fatty acid tail. The decapeptide has six diaminobutyric acid molecules (DAB), five of which are positively charged. Polymyxin B is composed of polymyxin B_1 and polymyxin B_2. Polymyxin B_1's tail is composed of 6-methyloctanoyl, and polymyxin B_2's tail is composed of 6-methylheptanoyl. F = phenylalanine, L = leucine, T = threonine.

Current-Voltage Relationship

The current-voltage relationship (*I-V*) of the PX induced conductance was determined using the protocol outlined by Tzan et al., (1993*a*). In brief, a control *I-V* relationship was first generated under voltage clamp conditions. Next, after PX had induced a significant increase in membrane conductance, the PX was washed out of the bath and an experimental *I-V* relationship was immediately generated. Because the apical membrane conductance is much smaller than the basolateral membrane conductance (for both control and experimental conditions) and PX did not alter the junctional conductance, one can calculate the current flowing through the induced conductance by subtracting the experimental current from the control current at each voltage step. The ionic selectivity of the induced conductance was then determined by curve fitting the current-form of the constant field equation to the data (*see* Tzan et al., 1993*a*).

Statistics

All data are expressed as the mean ±SE. Paired and unpaired Students t test were used to determine significance. $P < 0.05$ was considered statistically significant. Curve fitting of theoretical functions to the

data was performed using an IBM-based computer and the nonlinear curve-fitting routine NFit (Island Products, Galveston, TX).

Results

In this section it is first demonstrated that polymyxin B (PX) increases the transepithelial conductance of the rabbit urinary bladder epithelium. Next it is shown that the conductance increase is at the apical membrane, the conductance is permeable to monovalent anions and cations, and that the increase in conductance is dependent upon the apical membrane voltage, and the concentration of PX. Last, it is shown that PX is toxic to urinary bladder epithelial cells.

Effect of Polymyxin B on G_T

In previous studies (Tzan et al., 1993*a,b*, 1994; Kleine et al., 1995*a*) it was demonstrated that cationic polypeptides (e.g., protamine, polylysine, polyarginine and histones) increased the apical membrane conductance of the rabbit urinary bladder in a voltage-dependent manner, such that when the cell interior was made negative, the cationic polypeptides induced a change in G_t. In contrast, when the apical membrane potential was approximately 15 mV cell interior positive (a transepithelial voltage of −70 mV, serosa ground) the cationic polypeptide did not alter G_t (transepithelial conductance). An advantage of this voltage dependence is that it allows the kinetics of the conductance change to be determined without complications inherent in the diffusion of large molecules through an unstirred layer. A typical experimental protocol used in this study was to clamp the transepithelial voltage (V_t) at −70 mV, and then add 400 Units/ml (~36 μM) of PX to the mucosal bathing solution. After a 5-min incubation, V_t was clamped from −70 to 0 mV (an apical membrane voltage of −55 mV, cell interior negative) and the transepithelial conductance (G_t) measured. As shown in Fig. 2, at a V_t of −70 mV, PX did not alter G_t. However, when V_t was clamped to 0 mV (in the presence of mucosal PX), there was an increase in G_t. In the absence of mucosal PX, clamping V_t from −70 to 0 mV or from −70 to −110 mV did not result in a change in G_t (*data not shown*). Also illustrated in Fig. 2, is that the PX-induced conductance could be reversed by clamping V_t from 0 to −70 mV. The decrease in conductance had a biphasic time course composed of a near instantaneous decrease (i.e., complete in less that 1 sec), followed by a slower exponential like decrease in G_t with a rate constant of 0.054 ± 0.029 sec^{-1} ($n = 4$). The ratio of the rapid decrease in G_t to the slow decrease in G_t was 2.3 ± 0.3 ($n = 14$). Thus PX induces an increase in G_t in a voltage-dependent manner and this increase in G_t can be reversed by clamping V_t to −70 mV.

Site of Action of Polymyxin

The above data suggest that PX can increase the transepithelial conductance in a time-dependent and reversible manner. However, these data do not allow one to determine whether the increase in conductance was at the cell membrane or the tight junction. To determine the site of action, the method of Yonath and Civan (1971) was used. In brief, if PX increases only the cellular conductance, then a plot of the transepithelial conductance (G_t) *vs.* the short circuit current (I_{SC}) will be a straight line with an intercept equal to the tight junction conductance (G_j) and a slope equal to the inverse of the cellular electromotive force (E_c), where E_c is equal to the apical plus basolateral membrane electromotive force (E_a and E_{bl} respectively). If only G_j is altered, then G_t will increase in the absence of a change in I_{SC}. If both G_t and the cell conductance change, then the relationship will be curvilinear. As shown in Fig. 3, when V_t was clamped at 0 mV (thus the current being passed across the epithelium is equal to the current flow through the cell pathway, i.e., I_{SC}), there was a linear relationship between the PX-induced increase in transepithelial conductance (G_t) and the I_{SC}. The mean value for the inverse slope (E_c) was -41.1 ± 1.9 mV ($n = 6$). Since the basolateral membrane e.m.f. is ~−55 mV (Lewis et al., 1978), the PX-induced apical membrane e.m.f. is equal to 12.5 ± 2.1 mV (cell interior ground). Using the voltage form of the constant field equation and previously, determined intracellular ion activities (Lewis & Wills, 1981) in conjunction with the PX-induced apical membrane electromotive force gives a calculated value for Cl^- to K^+ permeability P_{Cl}/P_K of 1.7 ± 0.4 ($n = 5$). Thus PX introduces a nonselective pathway into the apical membrane of the urinary bladder epithelium.

Voltage Dependence of G_T

The above section demonstrated that when the apical membrane potential was clamped such that the cell interior was positive, PX did not alter the membrane conductance. However when V_t was clamped to 0 mV there was a rapid increase in conductance. Figure 4 shows the relationship between voltage and the PX-induced conductance. Axes for both V_t and the corresponding V_a (apical membrane voltage) are shown. The conversion of V_t to V_a assumes a constant V_{bl} (basolateral membrane voltage) of −55 mV (Lewis, Wills & Eaton, 1978). Of interest is that the increase in conductance is an exponential function of the membrane potential. The smooth curve through the data points is the best fit of Eq. 1 to the data.

$$\Delta G_t^{PX}(V) = \Delta G_t^{PX}(0)\exp^{(nVF/RT)} \quad (1)$$

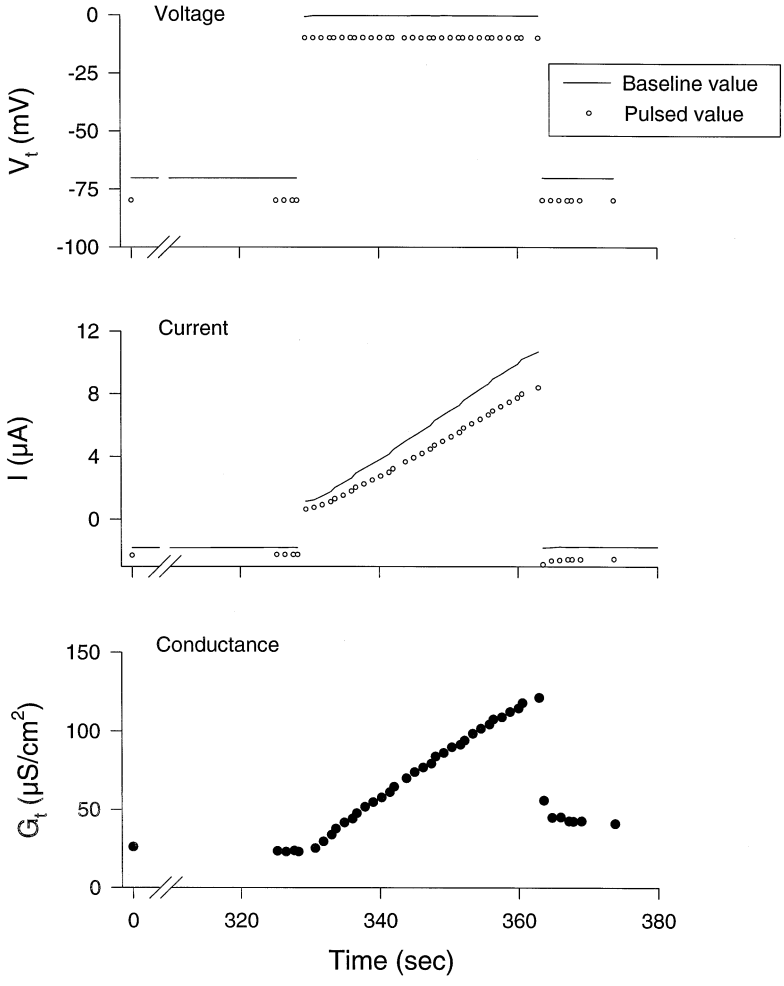

Fig. 2. At time 0, 400 Units/ml of polymyxin B was added to the mucosal bathing solution while the transepithelial voltage (V_t) was clamped at −70 mV (an apical membrane potential of approximately 15 mV cell interior positive). After a 5.5-min incubation, V_t was clamped at 0 mV, (the apical membrane potential was −55 mV, i.e., the cell interior was negative by 55 mV). There was a step increase in the transepithelial current (I) due to the Ohmic behavior of the tissue, which was followed by a linear increase in I. The small open circles represent the current response to a −10 mV voltage step of 30-msec duration. Note that the transepithelial conductance (G_t) did not change until the transepithelial voltage was clamped to 0 mV after which there was a linear increase in the conductance. When V_t was subsequently clamped to −70 mV, both current (I) and the transepithelial conductance returned to control values.

Where $\Delta G_t^{PX}(V)$ is the rate of increase of the PX-induced conductance as a function of voltage, $\Delta G_t^{PX}(0)$ is the rate of increase of the PX-induced conductance at zero voltage, V is the voltage, F is Faraday's constant, R is the gas constant, T is temperature in Kelvin and n is an empirical constant which determines the steepness of rise of the exponential function. The best fit value of n for PX was 1.24 ± 0.16 ($n = 4$). This value is not significantly different from the value of n reported by Tzan et al. (1993 *a,b*) for cationic polypeptides. Thus, as in previous studies of cationic proteins, we conclude that PX must ''sense'' an apical membrane voltage which must be cell interior negative in order for PX to induce an increase in the apical membrane conductance.

Kinetics of the PX-induced ΔG_T

At the beginning of the Results section it was shown that when V_t was clamped from −70 to 0 mV, in the presence of luminal PX, there was an increase in G_t (Fig. 2). It was noted that after V_t was clamped to 0 mV, there was a delay (up to 6 sec in duration) before G_t started to increase. To investigate this delay with increased time resolution; we recorded the time course of the PX-induced increase in transepithelial current at intervals ranging from 0.5 to 5 msec. In brief, the experimental protocol was to first measure the control transepithelial current (current in the absence of PX) as V_t was clamped from −70 to 0 mV. Next, the transepithelial current in

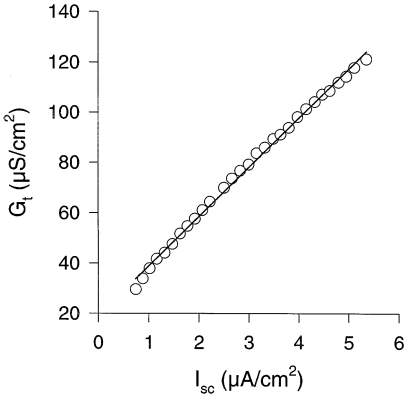

Fig. 3. This figure demonstrates the correlation between the PX-induced increase in transepithelial conductance (G_t) and the change in short circuit current (I_{SC}). The intercept of this plot is equal to the conductance of the tight junction (G_j; 20 μS/cm^2) and the slope is the inverse of the cellular e.m.f. (E_c; −51 mV). Of importance is that there is a linear relationship between G_t and I_{SC} which suggests that PX is altering (over a short time period) only the apical membrane conductance.

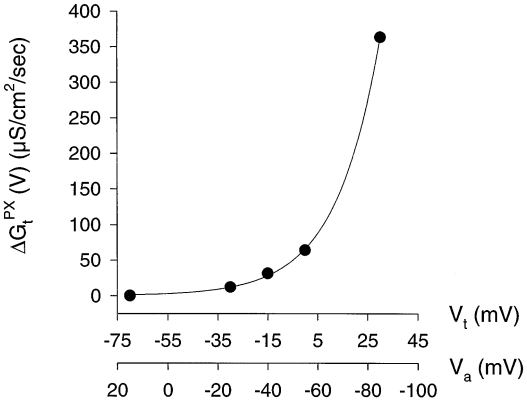

Fig. 4. An example of the voltage dependence of the PX-induced conductance. The smooth curve through the data points is the best fit of Eq. (1) to the data. The value for n in this example is 1.2. The apical membrane voltage (V_a) is calculated as $V_a = V_{bl} - V_t$, where the value of V_a uses the mucosal solution as 0 mV, V_{bl} is −55 mV and V_t is the transepithelial voltage (serosa ground). The ratio of apical to basolateral membrane conductance is 0.02, therefore V_{bl} will not change significantly as a function of V_t. At a clamped voltage of −70 mV, the cell interior is 15 mV positive relative to the mucosal solution.

the presence of luminal PX was recorded as V_t was clamped from −70 to 0 mV. The difference between the current in the presence of PX and the control (absence of PX) is then the time-dependent development of the PX-induced current. An example of the time course of the PX-induced current is illustrated in Fig. 5. As shown, there is no change in the current for approximately 0.1 sec, after which time the current increased, reaching a constant rate of change after ~0.5 sec. A simple model to describe the time course is:

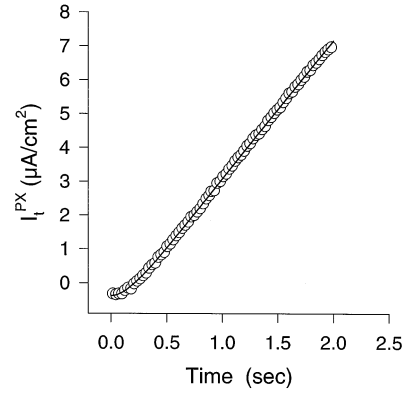

Fig. 5. Time course of the increase in the PX-induced transepithelial current (I_t^{PX}) when V_t was clamped from −70 to 0 mV (at time = 0) with a mucosal solution of 400 units/ml of PX. The data were collected at 5-msec intervals, however, for clarity this figure displays every fifth data point. Of interest is that there was a delay from when V_t was clamped to 0 mV and when the current started to increase in a linear manner. The smooth curve through the data is the best fit of Eq. 2 to the data. In this example, the best fit value for k_{ia} is 5.7 sec^{-1} (175 msec) and the ΔG_t^{PX} is 94 μS/cm^2 sec.

$$\text{Bath PX} \xrightarrow{\Delta G_t^{PX}} G_i^{PX} \xrightarrow{k_{ia}} G_t^{PX} \xrightarrow{k_{ao}}$$

where ΔG_t^{PX} is the rate of entry of PX into an inactive membrane-associated state (G_i^{PX}; an apical membrane cell negative voltage allows bath PX to interact with the apical membrane without causing an increase in membrane conductance), this inactive pool then enters the active state (G_t^{PX}) with a rate constant k_{ia}. The increase in the active conductance state was measured as the time dependent increase in the transepithelial current ($I_t^{PX}(t)$ when the transepithelial voltage (V_t) was clamped from −70 to −30 mV, 0, +30, or +50 mV. $I_t^{PX}(t)$ is equal to the product of $G_t^{PX}(t)$ and the net electrochemical gradient (Ψ_{ecg}) for ion flow across the apical membrane (Ψ_{ecg} is 15, 45, 75, or 95 mV cell interior ground, for a V_t of −30, 0, +30, or +50 mV respectively). Last, G_t^{PX} can exit the membrane with a rate constant of k_{ao}. The equation which describes this simple kinetic scheme is:

$$I_t^{PX}(t) = \Psi_{ecg}\,\Delta G_t^{PX}\left(\frac{1}{k_{ao}} + \frac{1}{k_{ia}-k_{ao}}\,e^{-tk_{ia}} - \frac{k_{ia}}{k_{ao}\,(k_{ia}-k_{ao})}\,e^{-tk_{ao}}\right) \quad (2)$$

The time-dependent increase in current when voltage clamping from −70 mV to less negative values was then curve fit by the above equation to estimate values for ΔG_t^{PX} and k_{ia} (k_{ao} was held at 0.022 sec^{-1}, *see* section on Reversal of PX-Induced Conductance for estimate of k_{ao}). Figure 6*a* shows that k_{ia} is proportional to ΔG_t^{PX} for varied PX concentrations, and clamp voltages. In

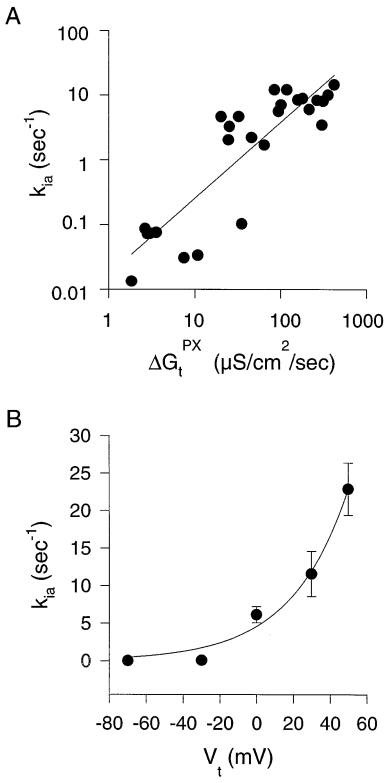

Fig. 6 (*A*) The relationship between the rate constant for entering the active state from the inactive state (k_{ia}) and the rate at which the conductance enters the inactive state from the bathing solution (ΔG_t^{PX}). These data represent different mucosal solution PX concentrations, different tissues, as well as different clamp potentials. (*B*) The relationship between k_{ia} and V_t. Note that k_{ia} increases as an exponential function of V_t. The smooth curve through the data is the best fit by a modified form of Eq. 1. Best fit value for k_{ia} (0) was 4.58 sec^{-1}, and for n was 0.9.

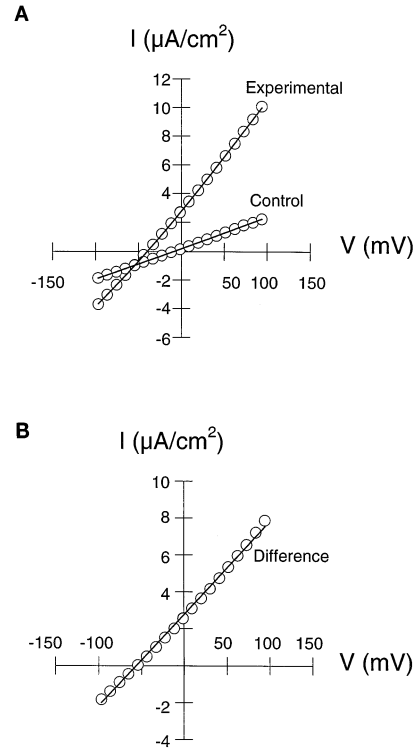

Fig. 7. Current-voltage relationship of the PX-induced conductance. (*A*) The control *I-V* relationship (*I-V* in the absence of bath PX) and the *I-V* after PX had induced a conductance and the PX then washed out of the bath (experimental). (*B*) The difference between experimental and control current at each clamp voltage. The smooth curve through the data points is the best fit of the constant field equation to the data. Best fit value for P_{Cl}/P_K is 0.47 ± 0.05 and for P_K is $2.26 \times 10^{-7} \pm 0.24 \times 10^{-8}$. *See* Materials and Methods for details of *I-V* relationship.

addition, k_{ia} is an exponential function of the transepithelial voltage (Fig. 6*b*). The best fit value to a modified form of Eq. 1 for $k_{ia}(0)$ was 4.58 sec^{-1} and for n was 0.9. These data suggest that upon changing to an apical membrane voltage which is cell negative, there are a number of kinetic steps that must be traversed before PX increases the membrane conductance and that at least one of these kinetic steps is voltage sensitive.

Selectivity of the Induced Conductance

To determine the ion selectivity of the PX-induced conductance, *I-V* relationships were performed before and after the addition of PX to the mucosal solution (Fig. 7*a*, *see* Materials and Methods for details). As shown in Fig. 7*b*, the current-voltage relationship resulting from the difference between the experimental and control current values has a curvilinear relationship. The zero current intercept was −57.1 ± 4.5 mV ($n = 4$) for PX in Ca^{2+}, Mg^{2+} free KCl Ringers and −45.5 ± 4.5 mV ($n = 4$) for Ca^{2+}, Mg^{2+}-free NaCl Ringers. The best fit of the current form of the constant field equation to the data yielded a P_K of $(3.0 \pm 0.45) \times 10^{-7}$ cm/sec ($n = 9$), a P_{Cl}/P_K of 0.51 ± 0.21 ($n = 5$) and a P_{Na}/P_K of 0.66 ± 0.1 ($n = 4$) for the PX-induced conductance. The intracellular ion activities used were those reported by Lewis and Wills (1981). Thus the PX-induced conductance is nonselective for cations over anions.

Did the intracellular ion concentrations change as a consequence of the PX-induced apical membrane conductance over the time period of the *I-V* measurements? To address this question we compared the value of E_c from the short term G_t *vs.* I_{SC} plots (10 sec) to the E_c values obtained from the *I-V* plots (2 min). There was no significant difference between these values (*data not shown*). This suggests that for a 2-min exposure to PX there is no measurable change in intracellular ion composition.

Reversal of the PX-induced Conductance

The PX-induced increase in G_t could be reversed by either clamping V_t back to −70 mV, or washing PX from the luminal solution.

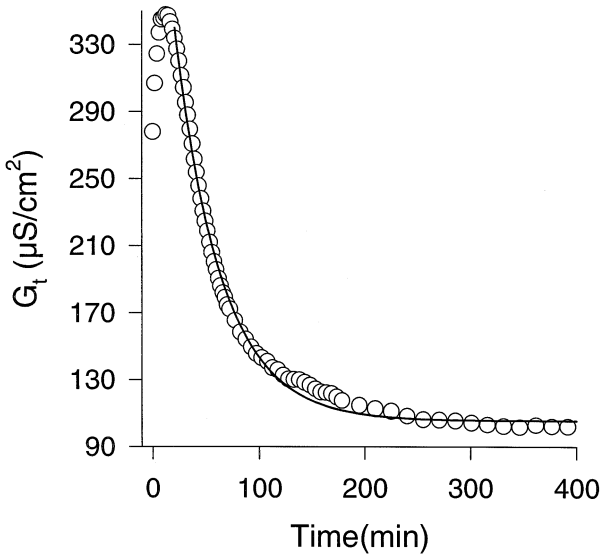

Fig. 8. The effect of removal of luminal PX (by washing) on the PX-induced conductance. In this experiment V_t was clamped to 0 mV in the presence of luminal PX. After a measurable increase in G_t, the PX was washed out of the luminal solution (starting at time zero) and G_t was monitored. Note that during the wash (which lasts for approximately 90 sec) G_t initially increased and then decreased. The initial increase in G_t (during washout of PX) is due to the time required to wash PX out of the bath as well as the time for the PX concentration in the unstirred layer to decrease. The smooth curve is the best fit of a single exponential to the data, with a rate constant of 0.023 sec^{-1}.

(i) Removal of bath PX: The linear increase in G_t induced by PX (when V_t was clamped from −70 to 0 mV, *see* Fig. 2) can be partially reversed by washing the luminal bath with a PX-free (Ca^{2+} and Mg^{2+}-free) KCl Ringers. Figure 8 shows a typical time course for the change in G_t during (and following) the removal of bath PX (by wash). The change in G_t was biphasic being composed of a conductance increase followed by a conductance decrease towards the control (pre-PX) G_t. G_t continued to increase for approximately 10 to 15 sec after the start of the luminal wash because of the time required for the PX concentration immediately adjacent to the apical membrane to decrease to zero. Thus during the initial phase of the wash period, PX was continuing to induce a conductance in the apical membrane. To estimate the rate of reversal (k_{ao}) of the PX-induced conductance by washing, a single inverse exponential was fit to the decreasing phase of the conductance change. The best fit value for k_{ao} (at a V_t of 0 mV) was 0.022 ± 0.003 sec^{-1} ($n = 11$). Thus in 45 sec the PX-induced conductance decreased by 63%. The peak value for the PX-induced conductance was 244 ± 47 μS/cm^2, and the PX-induced conductance which could not be washed out of the membrane was 68 ± 24 μS/cm^2. Thus removal of bath PX (in the absence of bath Ca^{2+} and Mg^{2+}) results in only a partial reversal of the PX-induced conductance. This residual PX-induced conductance can be removed from the apical membrane by washing the luminal chamber with a Ca^{2+} and Mg^{2+} containing KCl Ringers.

(ii) Voltage dependent reversal: The PX-induced conductance can also be reversed by voltage clamping the apical membrane potential to a cell positive value, i.e., clamping V_t from 0 to −70 mV (*see* Fig. 2). The decrease in G_t (when clamping from 0 to −70 mV) was biphasic with a rapid decrease (complete in less than 1 sec, representing a 65 ± 1.9% ($n = 20$) decrease of the induced conductance at a PX concentration of 400 Units/ml) followed by a slower exponential decrease to control values. Was the rapid decrease in conductance (when clamping V_t from 0 to −70 mV) due to the presence of bath PX? This question was addressed by measuring the PX-induced G_t in the presence and absence of bath PX at 0 mV (G_t^0) and then immediately after clamping V_t to −70 mV (G_t^{-70}). In the presence of bath PX (400 Units/ml) the ratio of the G_t^{-70}/G_t^0 was 0.35 ± .019, while in the absence of bath PX the ratio was 0.72 ± .016 ($n = 18$). Thus the magnitude of the decrease of the PX-induced G_t when clamping V_t from 0 to −70 mV was dependent upon whether PX was present in the bath.

PX Concentration: ΔG_t^{PX} and k_{ia}

Most of the above experiments were performed using 400 Units/ml of PX (this translates to a concentration of about 36 μM). In this section, we determine the dependence of the rate of the conductance increase (as well as k_{ia}, *see above*) on the luminal concentration of PX. The experimental protocol was to clamp V_t to −70 mV, and add PX to the luminal bath. After a 5-min incubation, V_t was clamped to 0 mV and the rate of conductance change and k_{ia} determined (*see* Eq. 2). Figure 9*a* and *b* shows that the rate of conductance change and k_{ia} were functions of luminal PX concentration. The concentration-conductance curve for PX is sigmoidal (Fig. 9*a*) suggesting that PX might associate with multiple binding sites before it can alter the apical membrane conductance. The data were fit by a kinetic scheme for multiple, highly cooperative sites (the Hill equation):

$$\Delta G_t^{PX}(PX) = \frac{\Delta G_t^{PX}(max)}{1 + \left(\frac{k_m}{[PX]}\right)^N} \quad (3)$$

where ΔG_t^{PX}(PX) is the rate of conductance change at a given concentration of PX, ΔG_t^{PX}(max) is the maximum rate of PX-induced conductance change, k_m is an apparent dissociation constant and N is the number of sites. The best fit value for k_m was 735 Units/ml, the normalized ΔG_t^{PX}(max) was 4.25 and the N was 1.7. This N suggests that more than one PX molecule is required to

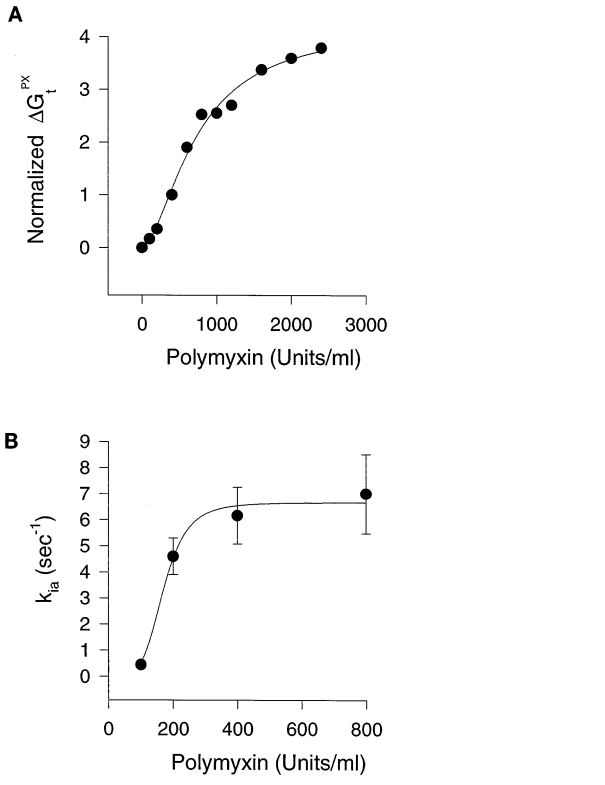

Fig. 9. (*A*) Concentration-conductance relationship for PX at a clamp voltage of 0 mV. The smooth curve through the data points is the best fit of a model for multiple, highly cooperative binding sites (*see* Eq. 3) and suggests that more than one PX molecule is required to induce a conductive unit. Because of variability among tissues to PX, the data were normalized to the conductance induced by 400 Units/ml of PX (the rate of conductance change at 400 Units/ml was 36.7 ± 7.3 μS/cm^2/sec, $n = 10$). G_t^{PX}(max) was then 156 μS/cm^2/sec, k_m was 735 Units/ml and N was 1.7. (*B*) Relationship between PX concentration and k_{ia}. The smooth curve through the data points is the best fit of the Hill equation (*see* Eq. 3), with an N of 4.6, k_m of 170 Units/ml and a maximum k_{ia} (k_{ia} (max)) of 6.7 sec^{-1} (a time constant of 150 msec) at a V_t of 0 mV.

induce a G_t^{PX}. The rate constant for entering the conductive state (k_{ia}) was also a sigmoidal function of PX concentration (Fig. 9*b*). Data were fit by the Hill equation yielding a value for k_m of 170 Units/ml, a N of 4.6 and a k_{ia} (max) of 6.7 sec^{-1} at a V_t of 0 mV.

Long-Term Effects of PX

In the first section of this paper we reported that the increase in G_t induced by PX could be reversed by washing PX out of the bathing solution, or voltage clamping the tissue such that the cell interior was positive. Such reversal was effective as long as the tissue was not exposed to mucosal PX for extended periods of time. To investigate the long-term effects of PX, tissues were exposed to PX for varying periods of time in Ca^{2+} and

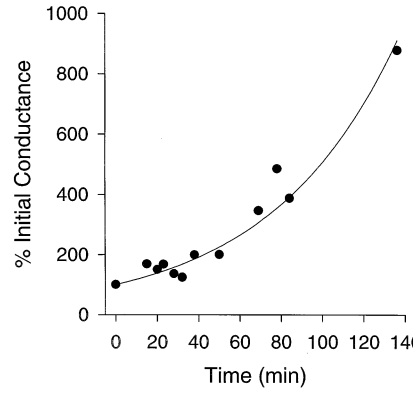

Fig. 10. The effect of long-term exposure of the urinary bladder epithelium to PX on the reversibility of the transepithelial conductance. Note that the longer the bladder is exposed to PX, the less reversible is the increase in the conductance. The smooth curve is the best fit of an exponential function to the data, with a best fit time constant of 62 mins.

Mg^{2+} containing KCl Ringers. After this time period PX was removed from the bath and the new steady-state conductance measured. Figure 10 demonstrates that the longer the urinary bladder epithelium was exposed to PX, the greater was the new steady-state conductance. These data suggest that there were long term effects of PX on epithelial integrity. The increase in conductance was not associated with an increase in the transport rate across the epithelium, which suggests that the gain of conductance was paracellular (increase in tight junctional conductance or loss of epithelial cells). The increase in conductance was well described by a single exponential with a time constant of 62 min for PX.

Discussion

In this section we first summarize the effects of luminal PX on the electrical properties of the urinary bladder epithelium. Next, these effects of PX on the bladder are compared to other cationic proteins as well as to the effects reported for PX on other biological systems. Last, a preliminary model is presented to describe how PX induces a conductance in the apical membrane of the urinary bladder epithelium.

Effect of PX on Bladder Epithelium

The data presented in this paper strongly suggest that PX increases the transepithelial conductance of the rabbit urinary bladder epithelium. The degree of the conductance increase was dependent upon the transepithelial voltage, the luminal concentration of PX, and the length of exposure to PX. At low concentrations of PX and short exposure times (typically less than a minute) at a

transepithelial potential of 0 mV, the subsequent removal of PX from the bath resulted in an almost complete return of the transepithelial conductance to control values. However, bladders exposed to high PX concentrations at a V_t of 0 mV for long periods of time, invariably had an increased transepithelial conductance which could not be completely reversed (*see* Fig. 10). The PX-induced conductance is nonselective, allowing the movement of both cations and anions. Given the nonselective nature of the PX-induced conductance, it is possible that the irreversible increase in the transepithelial conductance is due to the introduction of a paracellular conductance, produced by the influx of cations and anions leading to cell swelling and cell lysis.

PX was found to increase the apical membrane conductance only when the apical membrane voltage was cell interior negative. The time course of the increase in the membrane conductance had a delay (in which there was no conductance change) followed by an increase in conductance which became linear over time. This time course (particularly the delay) suggests that the formation of a conductance by PX is not a one-step process (e.g., closed to open) but rather that there are a number of intermediate nonconductive steps. In terms of a kinetic scheme these steps have been modeled to occur in series (*see* Eq. 2). This kinetic analysis suggests that the shorter the delay the greater was the rate of conductance increase. Both the rate of conductance change and the rate constant for entering the active state (k_{ia}) were exponential functions of the transepithelial potential, as well as sigmoidal functions of the bath PX concentration.

The magnitude of the induced conductance decrease, immediately after voltage clamping back to −70 mV (G_t^{-70}) from 0 mV (G_t^0), was dependent upon the presence of PX in the bath. If PX was washed out of the bath before clamping back to −70 mV, the ratio of the transepithelial conductances at −70 to 0 mV (G_t^{-70}/G_t^0) was 0.72. However, if the PX was not washed out of the mucosal bathing solution then the G_t^{-70}/G_t^0 was 0.35. Two possible explanations for this observation are: bath PX can block its own conductance in a voltage dependent manner, and the second is that the stability of the PX-induced G_t is a function of both membrane voltage and bath PX concentration. These two possibilities will be addressed in more detail below.

The dose-response curve for PX was sigmoidal in shape suggesting that more than one PX molecule is required to increase the membrane conductance. A model for multiple, highly cooperative sites, gave a binding coefficient of 1.7. Thus we speculate that at least 2 PX molecules are needed to produce a conductive unit.

Biology and Toxicology of PX

Because systemic administration of PX is nephrotoxic, it is presently restricted to external use or as a component of the irrigating solution used during long-term catheterization of the urinary bladder. Polymyxin B is a broad-spectrum antibiotic with a greater activity against gram-negative bacteria than gram-positive bacteria. Gram-negative bacteria have two series membranes, the outer and the cytoplasmic membrane, separated by the periplasmic space. The outer membrane in many gram-negative bacteria acts as an effective permeability barrier to hydrophobic molecules (e.g., antibiotics) as well as medium-to-large-sized hydrophilic molecules. Movement of small hydrophilic molecules (e.g., nutrients) occurs through porins (transmembrane pores) in the outer membrane.

Polymyxin's bactericidal action has two steps in gram negative bacteria. First it binds to the outer membrane and increases the permeability of this membrane (to hydrophobic molecules but not hydrophilic molecules) by an unknown mechanism. The increased outer membrane permeability then allows PX to enter the periplasmic space where it increases the permeability of the cytoplasmic membrane. It is this latter step which is lethal to the bacterium. Since PX increases the outer membrane permeability not only for itself, but also to small hydrophobic molecules, it enhances the bactericidal activity of other antibiotics. Bacteria with reduced levels of acidic lipopolysaccharide (LPS with lower total phosphate) in the extracellular leaflet of the outer membrane, are more resistant to the bactericidal activity of PX (Vaara & Viljanen, 1985; Storm et al., 1977; Vaara, 1992). This suggests that the outer membrane PX binding sites are the negatively charged phosphate groups on LPS.

The data in this paper are consistent with many of the observed effects of PX on the cytoplasmic membrane of bacteria. However, one apparent discrepancy is that the concentration of PX required to kill bacteria is 30-fold lower than that required to produce a measurable increase in the apical membrane permeability of the bladder epithelium. A similar lower sensitivity to PX was measured for an erythroleukemia cell line, K562 (Duwe et al., 1986). The difference of sensitivity between bacterial cells and mammalian cells can be accounted for by either a lower level of PX binding due to the lack of LPS in mammalian cell membranes or the difference in the membrane potential across a bacterial membrane (−200 mV, Alberts et al., 1989) compared to a mammalian cell (in this study −55 mV), and the voltage dependence of the PX-induced conductance (*see* Eq. 1). Thus at −200 mV the PX induced conductance would be 1,000 times greater than the conductance at −55 mV.

Cationic Proteins and Epithelial Integrity

There are numerous reports on the toxicity of cationic proteins to somatic cells. These cationic proteins fall

Table. Effect of cationic proteins on the mammalian urinary bladder

Protein	G_t	G_t *vs.* V_t	Reversible	Selectivity	Dose response	References
Protamine	$\uparrow G_a$	Exp.	Yes (voltage and wash)	Nonselective	M.M.	Tzan et al., 1993*a*,*b*,1994
Histone H1	$\uparrow G_a$	Exp.	Yes (voltage and wash)	Nonselective	Linear	Kleine et al., 1995*a*
Histone H5	$\uparrow G_a$	Exp.	Yes (voltage and wash)	Nonselective	Linear	Kleine et al., 1995*a*
Histone H4	$\uparrow G_a$	Exp.	Yes (voltage and wash)	Nonselective	M.M.	Kleine et al., 1995*a*
MBP	$\uparrow G_a$	Exp.	Yes (voltage and wash)	Nonselective	M.M.	Kleine et al., 1995*b*
EPO	$\uparrow G_a$	?	Yes (voltage and wash)	Nonselective	?	Kleine et al., 1995*b*
Polymyxin B	$\uparrow G_a$	Exp.	Yes (voltage and wash)	Nonselective	Sigmoidal	Present study

$\uparrow G_a$: the increase in G_t is at the apical membrane. Exp.: the increase in conductance as a function of voltage is exponential. Nonselective: permeable to both cations and anions. M.M.: dose-response best fit by Michaelis-Menten kinetics. Sigmoidal: dose response is described by a kinetic scheme with multiple, highly cooperative binding sites. Linear: there was a linear relationship between conductance and the concentration range tested.

into two groups, those whose physiological function is antimicrobial and those which were designed to perform other physiological functions. Proteins representative of the first category are: cationic protein (CAP) 37 and CAP 57, defensins (Kagan, Ganz & Lehrer, 1994), and cathepsin G from neutrophils (Spitznagel, 1990); major basic protein, eosinophil cationic protein, and eosinophil peroxidase from eosinophils (Gleich et al., 1993); magainins from glands in the frog skin (Zasloff, 1987); cryptdin from intestinal epithelial cells (Ouellette et al., 1992); TAP from tracheal epithelial cells (Diamond, Jones & Bevins, 1993); and α,β,γ thionins from the endosperm of certain plant seeds (Carrasco et al., 1981). Proteins in the latter category include, protamine sulfate (a DNA-compacting protein), and histones (giving tertiary structure to DNA). The effects of defensins have been studied on MDCK cells (Nygaard, Ganz & Peterson, 1993); MBP on urinary bladder (Kleine, Gleich & Lewis, 1995*b*) and trachea (Motojima et al., 1989; Jacoby et al., 1988); EPO on urinary bladder (Kleine et al., 1995*b*); cathepsin G on type II pneumocytes (Rochat et al., 1988); neutrophil proteins on endothelial monolayers (Peterson, Stone & Shasby, 1987); protamine on gallbladder (Bentzel et al., 1987; Poler & Reuss, 1987), proximal tubule (Sato & Ullrich, 1975), MDCK cells, T84 cells and HCT-8 cells (McEwan et al., 1993, Peterson & Gruenhaupt, 1990), descending loop (Koyama, Yoshitomi & Imai, 1991), urinary bladder (Parsons et al., 1990, Tzan et al., 1993*a*, 1994); and histones on urinary bladder epithelium (Kleine et al., 1995*a*). In almost all instances these proteins caused an increase in the transepithelial movement of both electrolytes and nonelectrolytes across the above epithelia. However, the primary site of action of these proteins was not determined for all of the above epithelia.

Recent studies on the mammalian urinary bladder, suggest there is a common mechanism by which these proteins can increase the transepithelial conductance (Table). In all cases the cationic proteins required a cell negative membrane potential before the protein could induce a conductance. The conductance could be reversed by removal of the protein from the bathing solution and was nonselective between cations and anions. Last, the site of action of these proteins was at the apical membrane. Differences among these proteins include, the time course of the conductance increase, the rate of reversal by either removal of bath protein or clamping the cell membrane potential to a positive value, as well as the ability of these proteins to block their own conductance (self-inhibition) in a voltage-dependent manner. As an example, the histone-induced conductance reached a plateau 20 sec after clamping V_t from −70 to 0 mV (Kleine et al., 1995*a*) as did the conductance induced by MBP (Kleine et al., 1995*b*). In contrast, the PX and PS induced conductances increased in a linear manner. The rate of reversal for MBP, histones and PX was rapid when the bath protein was removed, but was much slower for PS. In addition, neither histones (Kleine et al., 1995*a*) nor MBP (Kleine et al., 1995*b*) blocked their respective conductances i.e., there was no evidence of self-inhibition, while PS did exhibit self-inhibition.

The above discrepancies can be explained from the work by Tzan et al., (1993*a*,*b*). These authors found that those proteins with a lower (less than 50%) charge density (ratio of positively charged amino acids to total number of amino acids) induced a conductance which saturated over time while the molecules with a higher (greater than 50%) charge density induced a conductance which increased in a linear fashion over time. These differences in the time courses seem to be related to the rate of reversal of the conductance once the molecule has been removed from the bath. Proteins with low charge density reverse rapidly while those with high charge density reverse more slowly (Tzan et al., 1993*b*). PX has a charge density of 0.5, its conductance increase is linear as are the proteins with higher charge densities and its rate of reversal is rapid as are the proteins with lower charge densities. Tzan et al., (1993*a*), found that self-inhibition was linearly related to the protein's charge density (ratio of positively charged amino acids to total

number of amino acids). Proteins with a charge density of less than 0.5 were unable to demonstrate self-inhibition (MBP has a charge density of 0.145 and histones have charge densities which range from 0.22 to 0.35), while proteins with a charge density greater than 0.5 demonstrated progressively enhanced self-inhibition. Can the rapid decrease in G_t when clamping from 0 to −70 mV in the presence of bath PX be explained by self-inhibition? Using the linear relationship between charge density and % self-inhibition described above, a prediction of PX's self-inhibition can be made. At a V_t of −45 mV, a 20–25% decrease in G_t would be expected. However there was an ≈50% decrease in G_t when PX was present in the bath which suggests that most of the voltage-dependent decrease of the PX-induced conductance might not be due to self-inhibition.

Model for PX Conductance Formation

What is the mechanism by which PX can increase the conductance of a biological membrane? The greatest challenge in generating a model for PX-induced conductance formation is that PX is not long enough to span both monolayers which comprise the normal lipid bilayer (Hartmann, Galla & Sackmann, 1978). A number of mechanisms have been proposed. One is that PX displaces extracellular calcium or magnesium from the negatively charged lipids and this results in a destabilization of the membrane structure. This is an attractive possibility and is supported by observations in gram negative bacteria, where chelation of calcium and magnesium increased the outer membrane permeability of these bacteria as did the nonfatty acid containing nonapeptide of PX (Vaara, 1992). However, lipid bilayer studies do not support such a mechanism since the nonapeptide (PX without the fatty acid tail) was unable to alter bilayer conductance (while PX did alter the conductance of the lipid bilayer). An alternate mechanism was offered by Hartmann et al., (1978). These authors proposed that PX binds to negatively charged phosphate groups on lipids and thus causes a phase separation between the PX-bound lipid and the free lipid. The PX-bound lipid then produces a curvature in the membrane which acts as a pore (Hartmann et al., 1978). This pore formation was supported by lipid bilayer studies which demonstrated that PX produced channel-like opening and closing events (Schroder, Brandenburg & Seydel, 1992). What is not clear from this model is how generation of a curvature in one monolayer disrupts the transmonolayer conductivity. It is also not clear how such factors as membrane voltage, or the ability of bath PX to modify the PX-induced conductance in a voltage-dependent manner, can be incorporated into such a model.

A model for PX-induced conductance should include observations made in this paper. The concentration-conductance relationship saturated, which suggests a membrane binding site. This observation is in agreement with studies on both artificial lipid systems and bacteria. In addition, the dose-response curve suggests that at least two PX molecules are involved in the induction of a conductance. The lining of the conductive unit must be nonselective, this can be achieved by either a small diameter pore lacking a selectivity filter or a large diameter aqueous pore in which ions can traverse without interacting with the wall of the pore. Formation of a conductance has at least one voltage-dependent step. Finally, bath PX concentration rapidly reverses the PX-induced conductance in voltage-dependent manner.

A tentative model might include the following steps. First the PX binds to negatively charged membrane sites, possibly the phosphate group of phospholipids. The lipophilic tail then inserts into the nonpolar environment of the lipid bilayer. When the membrane voltage becomes cell negative, the surface PX molecules move further into the lipid bilayer and either open a pathway which spans both monolayers, or allow the movement of PX from the monolayer facing the extracellular compartment to the monolayer facing the intracellular compartment. In this latter instance, a single conductive unit is composed of two aligned PX hemipores, one in each lipid monolayer. Such a multistep model takes into account the time delay between voltage clamping the apical membrane potential and the appearance of an apical membrane conductance.

This work was supported by National Institute of Diabetes and Digestive and Kidney Diseases Grant DK-44821 and DK-51382.

References

Alberts, B., Bray, D., Lewis, J., Raff, M., Roberts, K., Watson, J.D. 1989. The Molecular Biology of the Cell. Garland Publishing, New York

Bentzel, C.J., Fromm, M., Palant, C.E., Hegel, U. 1987. Protamine alters structure and conductance of Necturus gallbladder tight junctions without major electrical effects on the apical membrane. *J. Membrane Biol.* **95:**9–20

Carrasco, L., Vazquez, D., Hernandez-Lucas, C., Carbonero, P., Garcia-Olmedo, F. 1981. Thionins: Plant peptides that modify membrane permeability in cultured mammalian cells. *Eur. J. Biochem.* **116:**185–189

Diamond, G., Jones, D.E., Bevins, C.L. 1993. Airway epithelial cells are the site of expression of a mammalian antimicrobial peptide gene. *P.N.A.S.* **90:**4596–4600

Duwe, A.K., Rupar, A., Horsman, G.H., Vas, S.I. 1986. In vitro cytotoxicity and antibiotic activity of polymyxin B nonapeptide. *Antimicrobial agents and Chemotherapy.* **30:**340–341

Gleich, G.J., Adolphson, C.R., Leiferman, K.M. 1993. The biology of the eosinophilic leukocyte. *Ann. Rev. Med.* **44:**85–101

Hartmann, W., Galla, H-J., Sackmann, E. 1978. Polymyxin binding to charged lipid membranes an example of cooperative lipid-protein interaction. *B.B.A.* **510:**124–139

Jacoby, D.B., Ueki, I.F., Widdicombe, J.H., Loegering, D., Gleich, G.J., Nadel, J.A. 1988. Effect of human eosinophil major basic protein on ion transport in dog tracheal epithelium. *Am. Rev. Respir. Dis.* **137:**13–16

Kagan, B.L., Ganz, T., Lehrer, R.I. 1994. Defensins: a family of antimicrobial and cytotoxic peptides. *Toxicology* **87:**131–149

Kleine, T.J., Gladfelter, A.S., Lewis, P.N., Lewis, S.A. 1995*a*. Histone-induced damage of a mammalian epithelium: the conductive effect. *Am. J. Physiol.* **268:**C1114–C1125

Kleine, T.J., Gleich, G.J., Lewis, S.A. 1995*b*. Both MBP and EPO increase epithelial permeability. *FASEB J.* **9:***A*5 (*Abst.*)

Koyama, S., Yoshitomi, K., Imai, M. 1991. Effect of protamine on ion conductance of upper portion of descending limb of long-loop nephron from hamsters. *Am. J. Physiol.* **260:**839–847

Lewis, S.A., Diamond, J.M. 1976. Na^+ transport by rabbit urinary bladder, a tight epithelium. *J. Membrane Biol.* **28:**1–40

Lewis, S.A., Eaton, D.C., Clausen, C., Diamond, J.M. 1977. Nystatin as a probe for investigating the electrical properties of a tight epithelium. *J. Gen. Physiol.* **70:**427–440

Lewis, S.A., Wills, N.K. 1981. Application and interpretation of Ion-specific microelectrodes in tight epithelia. *In:* The Application of Ion-Selective Microelectrodes. T. Zeuthen, editor. Elsevier/Noth-Holand Biomedical, Amsterdam, The Netherlands

Lewis, S.A., Wills, N.K., Eaton, D.C. 1978. Basolateral membrane potential of a tight epithelium: ionic diffusion and electrogenic pump. *J. Membrane Biol.* **41:**117–148

McEwan, G.T.A., Jepson, M.A., Hirst, B.H., Simmons, N.L. 1993. Polycation-induced enhancement of epithelial paracellular permeability is independent of tight junctional characteristics. *B.B.A.* **1148:**51–60

Motojima, S., Frigas, E., Loegering, D.A., Gleich, G.J. 1989. Toxicity of eosinophil cationic proteins for guinea pig tracheal epithelium *in vitro*. *Am. Rev. Respir. Dis.* **139:**801–805

Nygaard, S.D., Ganz, T., Peterson, M.W. 1993. Defensins reduce the barrier integrity of a cultured epithelium monolayer without cytotoxicity. *Am. J. Resp. Cell and Mol. Biol.* **8:**193–200

Ouellette, A.J., Miller, S.I., Henschen, A.H., Selsted, M.E. 1992. Purification and primary structure of murine cryptdin-I, a Paneth cell defensin. *FEBS lett.* **304:**146–148

Parsons, C.L., Boychuk, D., Jones, S., Hurst, R., Callahan, H. 1990. Bladder surface glycosaminoglycans: An epithelial permeability barrier. *J. Urol.* **143:**139–142

Peterson, M.W., Gruenhaupt, D. 1990. Protamine increases the permeability of cultured epithelial monolayers. *J. Appl. Physiol.* **68:**220–227

Peterson, M.W., Stone, P., Shasby, D.M. 1987. Cationic neutrophil proteins increase transendothelial albumin movement. *J. Appl. Physiol.* **62:**1521–1530

Poler, S.M., Reuss, L. 1987. Protamine alters apical membrane K and Cl permeability in gallbladder epithelium. *Am. J. Physiol.* **253:**C662–C671

Rochat, T., Casale, J., Hunninghake, G.W., Peterson, M.W. 1988. Neutrophil cathepsin G increases permeability of cultured type II pneumocytes. *Am. J. Physiol.* **255:***C*603–*C*611

Sato, K., Ullrich, K.J. 1975. Mechanism of inhibition of the proximal tubule isotonic fluids absorption by polylysine and other cationic polyamino acids. *J. Membrane Biol.* **21:**311–334

Schroder, G., Brandenburg, K., Seydel, U. 1992. Polymyxin B induces transient fluctuations in asymmetric planar lipopolysaccharide/phospholipid bilayers. *Biochem.* **31:**631–638

Spitznagel, J.K. 1990. Antibiotic Proteins of Human Neutrophils. *J. Clin. Invest.* **86:**1381–1386

Storm, D.R., Rosenthal, K.S., Swanson, P.E. 1977. Polymyxin and related peptide antibiotics. *Ann. Rev. Biochem.* **46:**723–763

Teichman, J.M.H., Abraham, V.E., Stein, P.C., Parsons C.L. 1994. Protamine sulfate and vancomycin are synergistic against staphylococcus epidermis prosthesis infection in vivo. *J. Urol.* **152:**213–216

Tzan, C.J., Berg, J.R., Lewis, S.A. 1993*a*. Effect of protamine sulfate on the permeability properties of the mammalian urinary bladder. *J. Membrane Biol.* **133:**227–242

Tzan, C.J., Berg, J.R., Lewis, S.A. 1993*b*. Modification of epithelial permeability by cationic polypeptides. *Am. J. of Physiol.* **265:***C*1637–*C*1647

Tzan, C.J., Berg, J.R., Lewis, S.A. 1994. Mammalian urinary bladder permeability is altered by cationic proteins: modulation by divalent cations. *Am. J. of Physiol.* **267:***C*1013–*C*1026

Vaara, M. 1992. Agents that increase the permeability of the outer membrane. *Microbiological Reviews.* **56:**395–411

Vaara, M., Viljanen, P. 1985. Binding of polymyxin B nonapeptide to gram-negative bacteria. *Antimicrobial agents and chemotherapy.* **27:**548–554

Yonath, J., Civan, M.M. 1971. Determination of the driving force of the Na^+ pump in toad bladder by means of vasopressin. *J. Membrane Biol.* **60:**105–128

Zasloff, M. 1987. Magainins, a class of anti-microbial peptides from *Xenopus* skin: isolation and characterization of two active forms and partial DNA sequence of precursor. *PNAS. USA.* **84:**5449–5453